

Fermi National Accelerator Laboratory

FERMILAB-Conf-98/113

Top Quark Physics at the Next Linear Collider

Rajendran Raja

*Fermi National Accelerator Laboratory
P.O. Box 500, Batavia, Illinois 60510*

April 1998

Published Proceedings of the *Workshop on Physics at the First Muon Collider and at the Front End of a Muon Collider*, Fermilab, Batavia, Illinois, November 6-9, 1997

Disclaimer

This report was prepared as an account of work sponsored by an agency of the United States Government. Neither the United States Government nor any agency thereof, nor any of their employees, makes any warranty, expressed or implied, or assumes any legal liability or responsibility for the accuracy, completeness, or usefulness of any information, apparatus, product, or process disclosed, or represents that its use would not infringe privately owned rights. Reference herein to any specific commercial product, process, or service by trade name, trademark, manufacturer, or otherwise, does not necessarily constitute or imply its endorsement, recommendation, or favoring by the United States Government or any agency thereof. The views and opinions of authors expressed herein do not necessarily state or reflect those of the United States Government or any agency thereof.

Distribution

Approved for public release; further dissemination unlimited.

Top quark physics at the Next Linear Collider

Rajendran Raja

*Fermi National Accelerator Laboratory
P.O. Box 500
Batavia, IL 60510*

Abstract. We report on the physics capabilities of a linear e^+e^- collider operating on or above the top quark threshold.

INTRODUCTION

The initial phase of the linear e^+e^- collider [1,2] is expected to operate at a maximum center of mass energy of 500 GeV, which will enable it to explore the threshold dependence of the $t\bar{t}$ cross section. Detailed exploration of the energy dependence of the $t\bar{t}$ cross section near threshold can lead to a determination of a number of important properties of the top quark, namely its mass m_t , its width Γ_t , the CKM matrix parameter V_{tb} , the Yukawa coupling of the top quark to the Higgs boson β_H , as well as the QCD coupling constant α_s . This is because the threshold shape depends on all these parameters. Measurements of the decay properties of the top quark will yield information on the form factors governing its decay. The ability to polarize the electron beam will aid significantly in suppressing WW backgrounds to the $t\bar{t}$ channel as well as help unravel the form factor information. In what follows, we will summarize this physics. A more detailed write-up can be found in Frey et al. [3].

TOP CROSS SECTION NEAR THRESHOLD

The standard model width of the top quark of mass $175 \text{ GeV}/c^2$ is $\approx 1.42 \text{ GeV}$. A $t\bar{t}$ (toponium) bound state will thus have at least twice the width of the top quark, since either of the top quarks may decay. The level spacing of toponia is $\approx \alpha_s^2 m_t$. For top quark masses greater than $150 \text{ GeV}/c^2$, the level spacing of toponia is comparable to the width of each state. This implies that

the S,P and D states of toponia form an indistinguishable enhancement below the $t\bar{t}$ threshold. The shape of this curve has been calculated using the Bethe-Salpeter equation by Strassler and Peskin [4] and has been extensively studied by others [5–9]. The shape depends on m_t and α_s . The greater α_s , the stronger the binding between $t\bar{t}$ pairs in the bound state and lower the position of the 1S state below threshold. The top cross section curve also depends on the top quark width and on the Higgs boson mass via the Yukawa coupling of the top quark and the Higgs boson. Figure 1(a) shows the theoretical top quark production cross section for a top quark mass of 175 GeV/c², infinite Higgs mass and $\alpha_s(M_Z^2) = 0.120$. At high energy, the center of mass energy resolution of e^+e^- colliders suffers from two effects, namely initial state radiation (ISR) and beamstrahlung. The effective QED expansion parameter at high energies for real photon emission is $\beta \equiv \frac{2\alpha}{\pi}(\ln(s/m_e^2) - 1) \approx 0.12$ (rather than α/π) for $\sqrt{s}=500$ GeV. For a muon collider of the same energy, β is 0.07, resulting in much smaller beam energy smearing due to ISR. Beamstrahlung, the emission of radiation by one beam due to the action on it of the other, is governed by the parameter $\Gamma \equiv \gamma(B/B_c)$, where B is the effective magnetic field strength of the beam ($\approx 6 \times 10^2$ T for NLC design) and $B_c \equiv m_e^2 c^3 / e \hbar \approx 4 \times 10^9$ T. This results in $\Gamma \approx 0.08$ at $\sqrt{s} = 500$ GeV for the SLAC NLC design. Figure 1(b) has ISR effects taken into account [10]. Figure 1(c) has ISR and beamstrahlung effects [11] taken into account. Figure 1(d) has in addition, single beam energy spreads appropriate to the SLAC NLC design applied. The energy spectrum of the beam may be characterized by a δ function piece at the nominal energy with a low energy tail due to the effects described above. The fraction of the luminosity in the δ function piece at $\sqrt{s}=500$ GeV for the SLAC X-band design is 43%. For a comparison of this curve with the corresponding one for the muon collider, please see the contribution by M. Berger to these proceedings [12].

At $\sqrt{s} = 500$ GeV, the lowest order total cross section for $m_t=180$ GeV/c² is 0.54 pb for unpolarized beams. One expects roughly 90% polarization for electrons at the NLC. The lowest order top cross section is 0.74pb(0.34pb) for fully left-hand (right-hand) polarized electron beam. For an integrated luminosity of 50fb⁻¹, achievable in one year's running, one expects roughly 25,000 $t\bar{t}$ events. The background to $t\bar{t}$ production is the production of W pairs. This process is dramatically reduced if the electron polarization is right handed.

Measurements of m_t and α_s at threshold

As α_s increases, the threshold bump of the theoretical curve moves lower. This can be compensated for by raising the top quark mass, resulting in a strong positive correlation between the fitted values of α_s and m_t . A number of studies have been performed to simulate measurements at the $t\bar{t}$ threshold.

A JLC study [9] assuming $m_t = 150 \text{ GeV}/c^2$ scans the threshold with 11 scan points of 1 fb^{-1} integrated luminosity per point. Assuming that the width of the top quark is given by the standard model, a simultaneous fit to α_s and m_t yields errors of 0.005 and $200 \text{ MeV}/c^2$ respectively. If one assumes that α_s is known from other sources to much better than this accuracy, one can fit for m_t alone yielding $100 \text{ MeV}/c^2$ for the top quark mass. An update for $m_t = 170 \text{ GeV}/c^2$ [13], yields errors of 0.007 and $350 \text{ MeV}/c^2$ for the same 11 point scan. A similar 10 point scan, with 5 fb^{-1} per point and $m_t = 180 \text{ GeV}/c^2$ [14], yields errors of 0.0025 and $120 \text{ MeV}/c^2$ for α_s and m_t respectively.

Measurements of top quark width and V_{tb}

Another quantity that contains information on α_s and Γ_t is the momentum distribution of the top quark pairs. After they are formed and move apart, the $t\bar{t}$ pairs are slowed down by the QCD potential. They decay before they have a chance to hadronize. The greater the value of α_s , the greater will be the QCD potential and the more the $t\bar{t}$ pairs will be slowed down. Similarly, the greater the value of Γ_t , the faster will be the decay and the greater the average momentum of the $t\bar{t}$ pair. This effect has been extensively studied theoretically [6,8] and phenomenologically [9,15]. A 100 fb^{-1} study of top momentum distributions yields an error on $\alpha_s = 0.00024$ (0.2%) and of 7% in Γ_t respectively. Another source of information on Γ_t is the threshold scan itself. Figure 2 shows the variation of the threshold curve as a function of Γ_t . Fujii et al [13] find that fixing α_s and fitting for m_t and Γ_t simultaneously for an 11 point scan with 1 fb^{-1} per point yields an error of $100 \text{ MeV}/c^2$ for m_t and a fractional error of 16 % for Γ_t . With a 50 fb^{-1} scan, the fractional error in Γ_t can perhaps be made as low as 5%.

In order to measure V_{tb} , one needs the partial width $\Gamma(t \rightarrow Wb)$. Knowing the total Γ_t , this can be determined by measuring the branching ratio $B(t \rightarrow Wb)$. No detailed Monte Carlos have been done to ascertain the precision to which this can be measured, but Frey et al [3] cite reasonable arguments to show that $B(t \rightarrow Wb)$ can be determined to a precision of 2.5% with 25 fb^{-1} of data, leading to a precision in V_{tb} of 2.8%.

Another quantity that is sensitive to the top quark width is the forward backward asymmetry of $t\bar{t}$ pairs [9,17]. This is caused by the interference between S, D states of toponium produced via the vector coupling of the γ/Z intermediate state and the P states produced by the axial vector coupling. The degree of forward backward asymmetry depends on the overlap of these states which in turn depends on Γ_t . This technique is less sensitive than the threshold scan (by a factor of 10 in luminosity), but provides a cross check of measurements made using other means.

Measurements of Higgs Yukawa coupling to the top quark

The $t\bar{t}$ pairs produced are subject not only to the QCD potential but also to a Yukawa potential V_H associated with Higgs exchange.

$$V_H = -\frac{\lambda_t^2}{4\pi} \frac{e^{-m_H r}}{r}$$

where m_H is the Higgs mass and the Yukawa coupling λ_t is given by

$$\lambda_t = \beta_H m_t / v_{Higgs}$$

v_{Higgs} is the Higgs vacuum expectation value. The dimensionless constant β_H is unity in the standard model but can assume other values in theories with more complicated Higgs structure. Figure 3 shows the variation of the standard model top cross section for various values of the Higgs mass [16]. If one assumes that the Higgs boson has been discovered by the time the NLC turns on, then one can use the NLC to measure deviations in β_H from unity. Figure 4 shows the variation of the top cross section as a function of β_H , with all the beam effects included. Fujii et al [13] apply their 11 point scan method to show that with 11 fb^{-1} of data it is possible to determine β_H to 25% for $m_t=170 \text{ GeV}/c^2$.

It should also be possible to measure the Higgs Yukawa coupling by observing the direct emission of a Higgs boson associated with $t\bar{t}$ production if the center of mass energy is sufficient to allow such “higgsstrahlung” .

FORM FACTORS AND DECAY DISTRIBUTIONS

Another rich source of information on the properties of top quarks is their decay modes and distributions. The search for rare decay modes of the top quark is perhaps better done in hadron machines with much larger rates of $t\bar{t}$ production. However, the existence of polarization and an initial state of well defined energy provide the lepton colliders with perhaps a unique means to explore the decay dynamics of top quarks.

The top neutral-current coupling can be generalized to the following form for the γ/Z - t - \bar{t} or vertex factor:

$$\begin{aligned} \mathcal{M}^{\mu(\gamma,Z)} = & e\gamma^\mu \left[Q_V^{\gamma,Z} F_{1V}^{\gamma,Z} + Q_A^{\gamma,Z} F_{1A}^{\gamma,Z} \gamma_5 \right] \\ & + \frac{ie}{2m_t} \sigma^{\mu\nu} k_\nu \left[Q_V^{\gamma,Z} F_{2V}^{\gamma,Z} + Q_A^{\gamma,Z} F_{2A}^{\gamma,Z} \gamma_5 \right] , \end{aligned}$$

which reduces to the SM tree level expression with the form factors $F_{1V}^\gamma = F_{1V}^Z = F_{1A}^Z = 1$ and the others zero. The quantities $Q_{A,V}^{\gamma,Z}$ are the SM coupling

Form Factor	SM Value (Lowest Order)	Limit 68% CL	Limit 90% CL
$F_{1R}^W(P=0)$	0	± 0.13	± 0.18
$F_{1R}^W(P=80\%)$	0	± 0.06	± 0.10
F_{1A}^Z	1	1 ± 0.08	1 ± 0.13
F_{1V}^Z	1	1 ± 0.10	1 ± 0.16
F_{2A}^γ	0	± 0.05	± 0.08
F_{2V}^γ	0	± 0.07	$^{+0.13}_{-0.11}$
F_{2A}^Z	0	± 0.09	± 0.15
F_{2V}^Z	0	± 0.07	± 0.10
$\Im(F_{2A}^Z)$	0	± 0.06	± 0.09

TABLE 1. The upper and lower limits of the couplings in their departures from the SM values are given at 68% and 90% CL. All couplings, each with real and imaginary parts, can be determined in this way. The right-handed charged-current coupling is shown both for unpolarized and 80% left-polarized electron beam, whereas the other results assume 80% left-polarized beam only. \Im is the imaginary part, otherwise the results listed here are for the real parts.

constants: $Q_V^\gamma = Q_A^\gamma = \frac{2}{3}$, $Q_V^Z = (1 - \frac{8}{3} \sin^2 \theta_W)/(4 \sin \theta_W \cos \theta_W)$, and $Q_A^Z = -1/(4 \sin \theta_W \cos \theta_W)$. The non-standard couplings $F_{2V}^{\gamma,Z}$ and $F_{2A}^{\gamma,Z}$ correspond to electroweak magnetic and electric dipole moments, respectively. For the top charged-current coupling we can write the W - t - b vertex factor as

$$\mathcal{M}^{\mu,W} = \frac{g}{\sqrt{2}} \gamma^\mu \left[P_L F_{1L}^W + P_R F_{1R}^W \right] + \frac{ig}{2\sqrt{2} m_t} \sigma^{\mu\nu} k_\nu \left[P_L F_{2L}^W + P_R F_{2R}^W \right],$$

where the quantities $P_{L,R}$ are the left-right projectors. In the SM we have $F_{1L}^W = 1$ and all others zero. The form factor F_{1R}^W represents a right-handed, or $V + A$, charged current component. Using an integrated luminosity of 10 fb^{-1} , and the $t\bar{t}$ decay mode final state of lepton + jets, and an electron polarization of $\pm 80\%$, it can be shown [18,19] that the form factors given above can be determined to a precision shown in table 1 at a center of mass energy of 500 GeV.

CONCLUSIONS

The e^+e^- linear colliders (and the muon collider) offer an excellent means of probing the physics of the $t\bar{t}$ threshold and extracting fundamental parameters

such as m_t , Γ_t , β_H as well as the form factors governing top decay to precisions difficult to attain using hadron machines.

REFERENCES

1. C. Adolphsen, *et al.*, "Zeroth-Order Design for the NLC", SLAC Report 474, May 1996 may be found at <http://www.slac.stanford.edu/accel/nlc/zdr/>
2. JLC-I, KEK report 92-16 can be found at <http://www-jlc.kek.jp/JLC.proposal-e.html>
3. Top quark Physics: Future measurements, R.Frey et al, Fermilab-CONF-97-085, Apr 1997, LANL e-print Archive hep-ph/9704243, Proceedings of the 1996 DPF/DPB Summer Study on New directions for High Energy Physics, Snowmass Colorado.
4. M. Strassler and M. Peskin, Phys. Rev. **D43**, 1500 (1991).
5. V. Fadin and V. Khoze, JETP Lett. **46**, 525 (1987) and Sov. J. Nucl. Phys. **48**, 309 (1988).
6. M. Jezabek, J. Kuhn, and T. Teubner, Z. Phys. **C56**, 653 (1992).
7. M. Jezabek and T. Teubner, Z. Phys. **C59**, 669 (1993).
8. Y. Sumino, K. Fujii, K. Hagiwara, H. Murayama, and C.-K. Ng, Phys. Rev. **D47**, 56 (1993).
9. K. Fujii, T. Matsui, and Y. Sumino, Phys. Rev. **D50**, 4341 (1994).
10. E.A. Kuraev and V.S. Fadin, Sov. J. Nucl. Phys. **41**, 466 (1985).
11. Pisin Chen, Phys. Rev. **D46**, 1186 (1992).
12. "The $t\bar{t}$ threshold at Muon Colliders", M.Berger, these proceedings.
13. K. Fujii, proceedings of the 1995 SLAC Summer Institute.
14. P. Comas, R. Miquel, M. Martinez, and S. Orteu, "Recent Studies on Top Quark Physics at NLC", proceedings of the Workshop on Physics and Experiments with Linear Colliders (LCWS95), 1995.
15. P. Igo-Kemenes, M. Martinez, R. Miquel, and S. Orteu, proceedings of the Workshop on Physics and Experiments with Linear Colliders (LCWS93), Waikoloa, Hawaii, USA, 1993.
16. R. Harlander, M. Jezabek, and J.H. Kuhn, Acta. Phys. Polon. **27**, 1781 (1996), hep-ph/9506292 (1995).
17. H. Murayama and Y. Sumino, Phys. Rev. **D47**, 82 (1993).
18. R. Frey, "Top Quark Physics at a Future e^+e^- Linear Collider: Experimental Aspects," proceedings of the Workshop on Physics and Experiments with Linear Colliders (LCWS95), Iwate, Japan, Sept., 1995; hep-ph/9606201 (1996).
19. M. Fero, Proceedings of the 1996 DPF/DPB Summer Study on New directions for High Energy Physics, Snowmass Colorado.

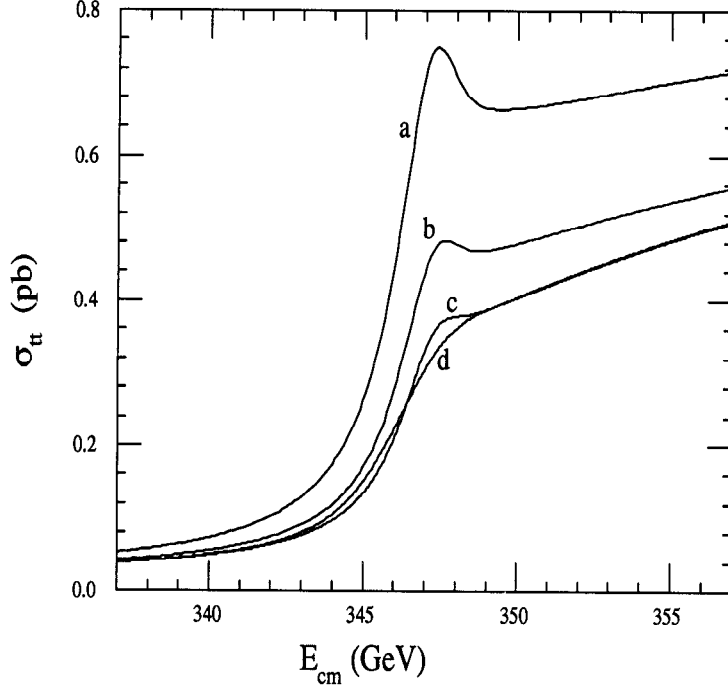


FIGURE 1. Production cross section for top-quark pairs near threshold for $m_t = 175$ GeV^2 . The theoretical cross section is given by curve (a). The following energy redistribution effects have been applied to the theory for the remaining curves: (b) initial-state radiation (ISR); (c): ISR and beamstrahlung; (d): ISR, beamstrahlung, and single-beam energy spread.

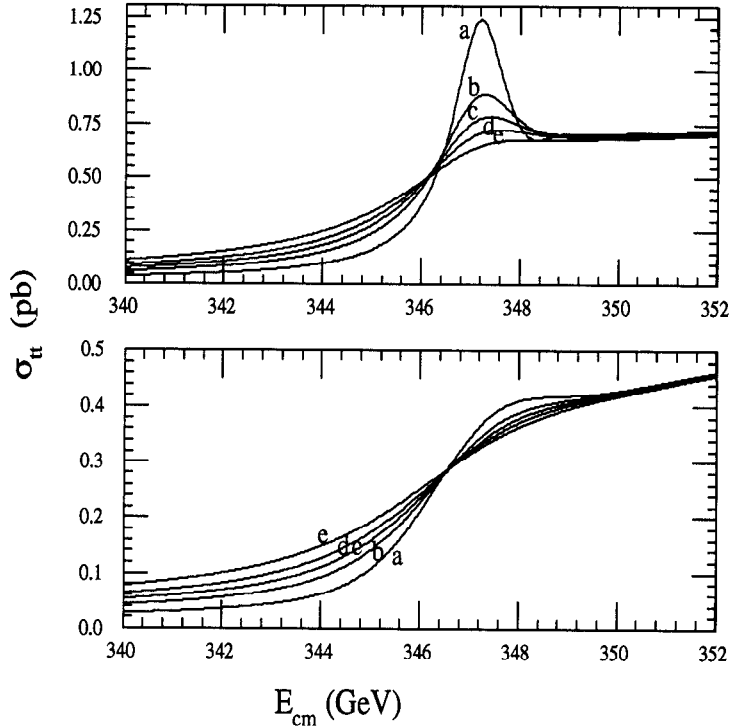


FIGURE 2. Threshold shape for various values of Γ_t . The upper plot is the theoretical prediction, while the lower plot includes all radiative and beam effects. The different curves correspond to $\Gamma_t/\Gamma_t^{\text{SM}} =$ (a) 0.5, (b) 0.8, (c) 1.0, (d) 1.2, and (e) 1.5. We assumed $m_t = 175$ GeV , where the Standard Model width is $\Gamma_t^{\text{SM}} = 1.42$ GeV .

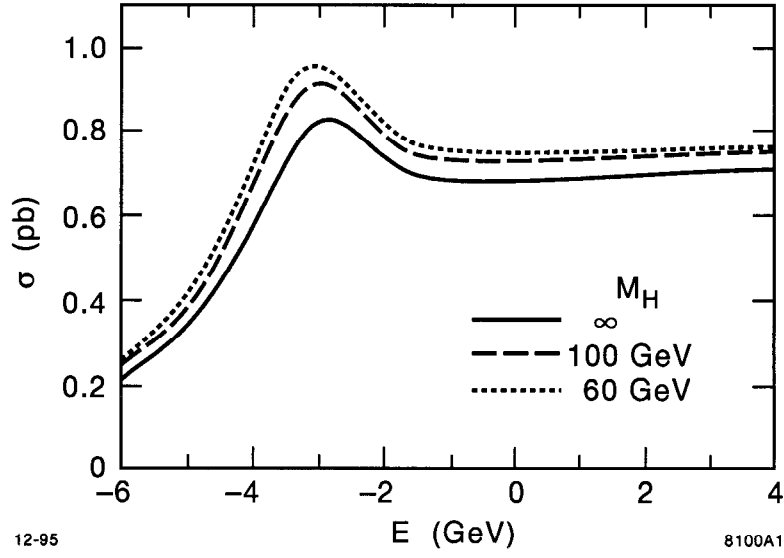


FIGURE 3. Cross section near threshold for different Higgs masses due to the Yukawa potential. $m_t = 180 \text{ GeV}/c^2$ was assumed. The abscissa center-of-mass energy is relative to $2m_t$.

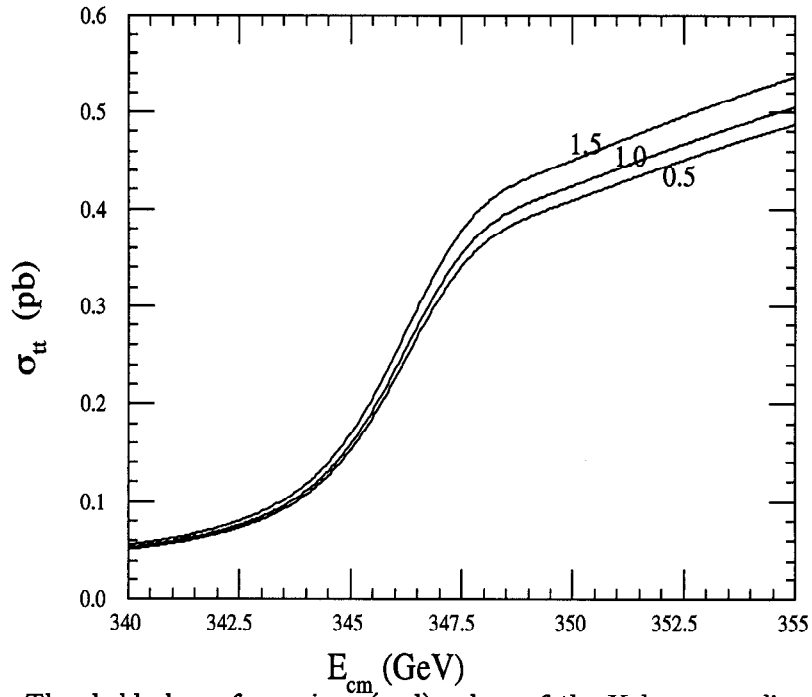


FIGURE 4. Threshold shape for various (real) values of the Yukawa coupling strength β_H . All radiative and beam effects are included, and $m_t = 175 \text{ GeV}$, $m_H = 300 \text{ GeV}$ are used. The different curves correspond to $\beta_H = 1.5, 1.0$, and 0.5 , as indicated.